

See discussions, stats, and author profiles for this publication at: <https://www.researchgate.net/publication/272843887>

# Bioinspired Polydopamine Sheathed Nanofibers for High-Efficient in Vivo Solid-Phase Microextraction of Pharmaceuticals in Fish Muscle

ARTICLE in ANALYTICAL CHEMISTRY · FEBRUARY 2015

Impact Factor: 5.64 · DOI: 10.1021/ac5048357 · Source: PubMed

---

CITATIONS

4

---

READS

68

7 AUTHORS, INCLUDING:



Jianqiao Xu

Sun Yat-Sen University

16 PUBLICATIONS 134 CITATIONS

SEE PROFILE



Ruifen Jiang

Sun Yat-Sen University

37 PUBLICATIONS 313 CITATIONS

SEE PROFILE



Gangfeng Ouyang

Sun Yat-Sen University

109 PUBLICATIONS 2,295 CITATIONS

SEE PROFILE

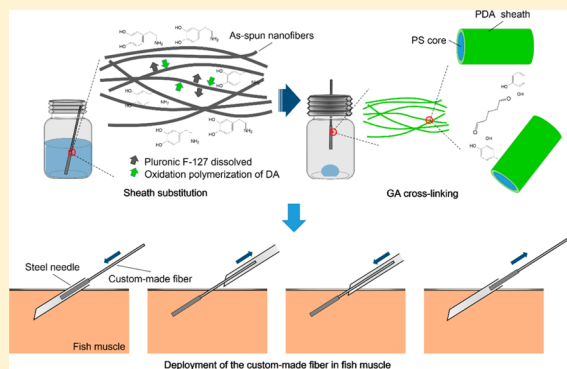
# Bioinspired Polydopamine Sheathed Nanofibers for High-Efficient in Vivo Solid-Phase Microextraction of Pharmaceuticals in Fish Muscle

Jianqiao Xu, Shuyao Huang, Rongben Wu, Ruifen Jiang,\* Fang Zhu, Jing Wang, and Gangfeng Ouyang\*

MOE Key Laboratory of Aquatic Product Safety/KLGHEI of Environment and Energy Chemistry, School of Chemistry and Chemical Engineering, Sun Yat-sen University, Guangzhou, Guangdong 510275, China

## S Supporting Information

**ABSTRACT:** In this study, electrospun nanofibers were used as solid-phase microextraction (SPME) fiber coatings after substituting the water-soluble sheath of the emulsion electrospun polystyrene (PS) @Pluronic F-127 core–sheath nanofibers with biocompatible and water-stable polydopamine (PDA) and subsequently being appropriately cross-linked with glutaraldehyde (GA) to enhance the strength of the electrospun architecture. The novel custom-made PS@PDA-GA coating was wettable in aqueous solutions and thus exhibited much higher extraction efficiency than the nonsheathed PS nanofiber coating and the thicker polydimethylsiloxane (PDMS) coating. The novel coating also possessed excellent stability (relative standard deviations (RSDs) less than 7.3% for six sampling-desorption cycles), interfiber reproducibility (RSDs less than 14.3%), and antibiofouling ability, which were beneficial for in vivo sampling. The PS@PDA-GA fiber was used to monitor pharmaceuticals in dorsal-epaxial muscle of living fish, and satisfactory sensitivities with the limits of detection in the range of 1.1 (mefenamic acid) to 8.9 (fluoxetine)  $\text{ng}\cdot\text{g}^{-1}$  and comparable accuracies to liquid extraction were achieved. In general, this study explored a convenient and effective method to sheath nanofibers for high-efficient in vivo SPME of analytes of interest in semisolid tissues.



In vivo solid-phase microextraction (SPME) has been a very popular sampling and sample preparation method for detecting analytes of interest in living biotas in recent years.<sup>1</sup> Since its conception, the new exploration of in vivo SPME on clinical analysis,<sup>2</sup> pollutant detection,<sup>3</sup> metabolomics detection,<sup>4</sup> and central nervous system studies<sup>5</sup> continuously inspires the scientific communities. The advantages of in vivo SPME relative to other in vivo analytical methods have been well demonstrated in the literature,<sup>1–5</sup> while it has long been a task concerning the scientific communities that the sampling duration of in vivo SPME should be shortened, which is not only critical for promoting analytical efficiency<sup>6–8</sup> but also intriguing for providing a glimpse of the short-term events proceeding in dynamic biological systems.<sup>9</sup> The development of calibration methods for pre-equilibrium in vivo SPME offers theoretical backgrounds for cutting down sampling durations,<sup>6–8</sup> but the accompanied loss of sensitivity is troublesome.<sup>9</sup> In particular in the semisolid tissues, the sampling kinetics of SPME is dramatically slowed down due to the tortuous diffusion paths.<sup>10</sup>

Designing SPME probes for in vivo sampling with high specific surface areas can accelerate the sampling kinetics.<sup>11</sup> Even though thin-film SPME samplers have been used in detecting human skin volatiles,<sup>12</sup> they are difficult to be deployed in tissues or blood vessels to sampling analytes therein. Nanomaterials are also used in SPME fiber coatings to accelerate the sampling kinetics and increase the loading

capacities.<sup>13,14</sup> However, some fiber preparation methods such as the sol–gel method seem to not make the best use of nanomaterials, as the surface areas of the fibers were not effectively increased since the dominant fractions of nanomaterials were encased in gel;<sup>15</sup> besides, the adsorption sites of the coatings might not be fully accessible, as the diffusion paths are very tortuous in the coatings and the pores may be blocked by highly stacking architectures and by trapped air.<sup>16</sup> In addition, it is highly remarkable that the potential toxic effects of nanomaterials should be quite known prior to in vivo applications, in case of exfoliation of nanomaterials from the coatings.<sup>17–19</sup>

Very recently, Wu et al. prepared nanofibers with a biocompatible and wettable sheath for microextraction of pharmaceuticals in an aqueous biological matrix.<sup>20</sup> For the 3D-interconnected and wettable pores, the air trapped in the pores could be expelled out by tissue fluids; therefore, the surfaces of the nanofibers were fully accessible. It was observed that the sampling kinetics of the nanofibers in rabbit blood was quite rapid and that it took only several minutes to reach the sampling equilibrium. However, coaxial electrospinning was much more complicated than single-spinneret electrospinning,

Received: December 26, 2014

Accepted: February 25, 2015



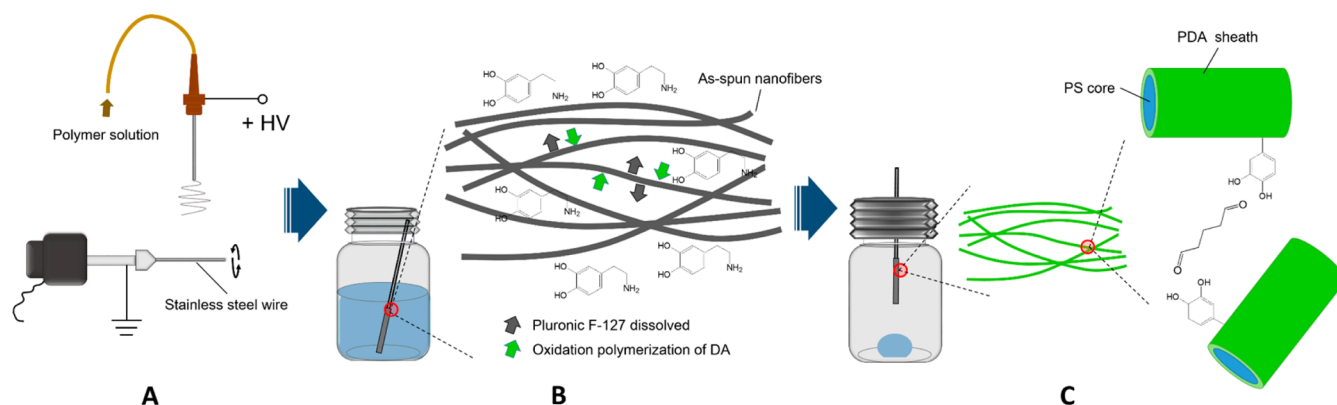


**Figure 1.** Flow diagram of the preparation of the novel SPME fiber. Electrospinning of PS/Pluronic F-127 blend solution on a SSW (A), polymerization of DA on the surfaces of the as-spun nanofibers as simultaneously Pluronic F-127 was dissolved (B), and cross-linking of the PDA sheathed nanofibers in GA vapor (C).

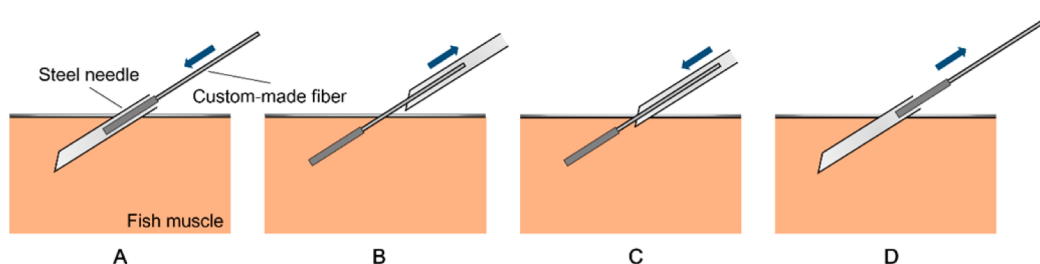


**Figure 2.** Deployment of PS@PDA-GA fiber in fish muscle. Deploy PS@PDA-GA fiber under the guidance of a steel needle (A), remove the steel needle and expose the custom-made fiber in fish muscle (B), carefully put back the steel needle in the fish muscle at the end of sampling (C), and remove the custom-made fiber (D).

as viscosities of core and sheath solutions need to be well controlled, and infusion of core and sheath solutions need to be avoided.<sup>21</sup> In addition, the sheath material used was expensive, and additional cross-linking in the sheath was inevitable to improve the stability of the sheath in water. Moreover, sampling with the nanofiber mat could only be realized under the assistance of a microfluidic device, and blood needed to be withdrawn out of the rabbit body. Sampling in the semisolid tissues with the nanofiber mat was even impractical. Therefore, developing a more convenient and inexpensive sheathing method is necessary; meanwhile, developing the nanofibers into SPME fibers might facilitate direct sampling in biological matrices.

Bioinspired polydopamine (PDA) was recently demonstrated to be capable of self-coating nearly all kinds of surfaces.<sup>22</sup> Enlightened by the previous studies of modifying surfaces of microfibers and nanofibers with PDA,<sup>23–25</sup> in the present study, electrospun nanofibers were collected on stainless steel wires, and PDA self-sheathing of the electrospun nanofibers and glutaraldehyde (GA) cross-linking were subsequently followed. For promoting PDA sheathing efficiency, an innovative sheath-substitution methodology was also proposed. Due to the biocompatible and hydrophilic nature of PDA, PDA sheathed nanofibers are promising for high-efficient sampling of target analytes in biological matrices. The nanofibers were then successfully used to directly sample basic and acidic pharmaceuticals in fish dorsal-epaxial muscle.

## EXPERIMENTAL SECTION

**Chemicals and Materials.** Fluoxetine (FLX), norfluoxetine (NFLX), and the deuterated standards, fluoxetine-*d*<sub>3</sub> and norfluoxetine-*d*<sub>3</sub>, were purchased from Toronto Research

Chemical Inc. (New York, ON, Canada). Tolfenamic acid (TOLF), mefenamic acid (MEF), flufenamic acid (FLUF), and gemfibrozil (GEMF) were all purchased from Tokyo Chemical Industry Co. Ltd. (Tokyo, Japan). Polystyrene (PS, molecular weight ~280 000), Pluronic F-127, dopamine hydrochloride, HPLC grade methanol, and tri(hydroxymethyl)aminomethane hydrochloride (Tri buffer) were purchased from Sigma-Aldrich Co. Ltd. (St. Louis, USA). Stainless steel wires (SSWs, 480  $\mu\text{m}$  in diameter, medical grade) were purchased from Small Parts Inc. (Miami Lakes, USA). Aqueous GA solution (50%) was purchased from Aladdin Reagent Company (Shanghai, China). *N,N*-Dimethylformamide and chloroform were purchased from Guangzhou Chemical Factory (Guangzhou, China).

**Animals and Exposure.** Immature tilapias (*Oreochromis mossambicus*) were purchased from a local fishery. Tilapias were reared in aerated 80 L aquaria containing 40 L of dechlorinated tap water for 2 weeks before experiment. Then, the fish were divided into two groups ( $n = 6$  for each) and exposed to spiked tap water for 10 days at two different levels. Briefly, 40 L of water was spiked with an aliquot of 80 or 400  $\mu\text{L}$  of stock solution (1000  $\mu\text{g}\cdot\text{mL}^{-1}$  for each pharmaceutical, in methanol). The nominal water concentrations were 2.0 and 10.0  $\mu\text{g}\cdot\text{L}^{-1}$ . In order to keep the water concentration steady, water was changed with fresh tap water and respiked with the initial amounts every 12 h. The water quality was monitored daily (pH 6.5, dissolved oxygen  $6.5 \pm 0.2$  ppm, and temperature  $27.3 \pm 1.3$  °C). Prior to in vivo SPME, the lengths and weight of the fish were recorded (length 11.2 to 12.7 cm, median 12.1 cm; weight 27.0 to 37.0 g, median 29.5 g). All the animal experiments were approved by the Animal Ethical and Welfare Committee of Sun Yat-sen University.

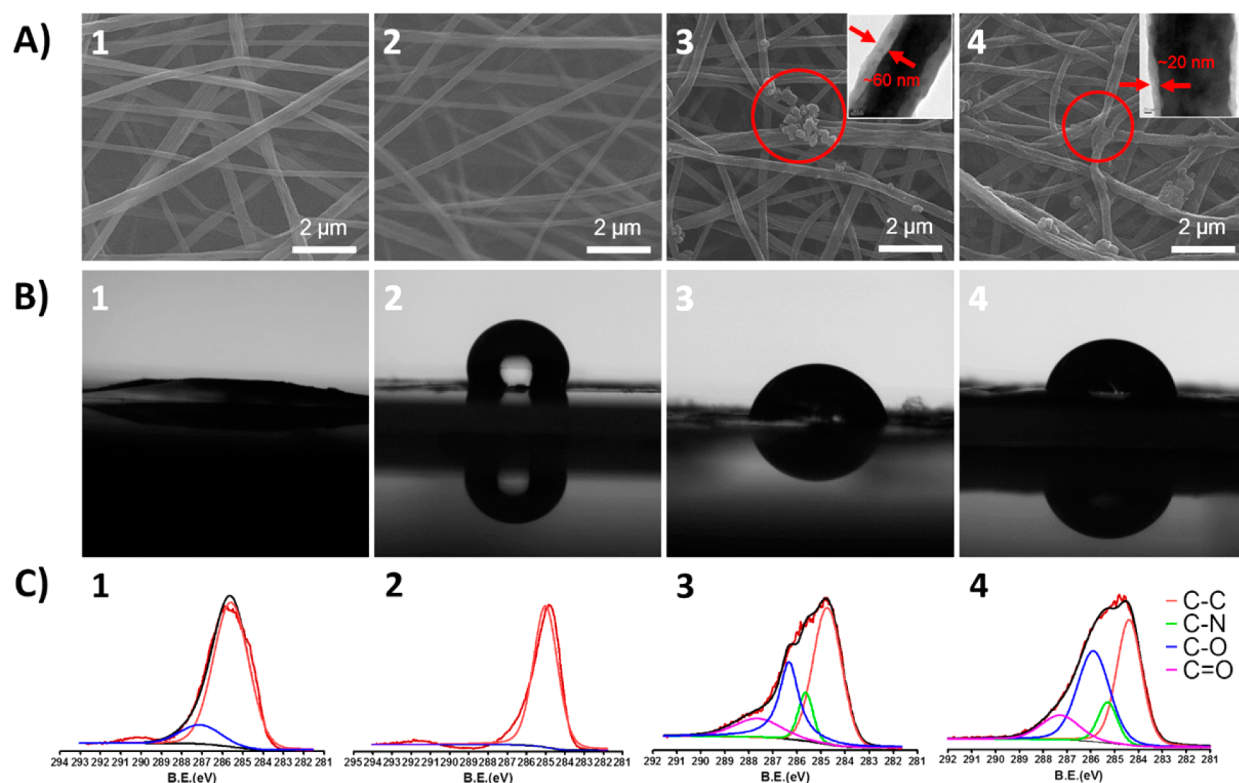


**Figure 3.** SEM images (A), contact angles (B), and peak fitting of C 1s XPS spectra (C) of the as-spun (1), water washed (2), PDA sheathed (3), and GA cross-linked (4) nanofibers. The insets in A-3 and A-4 were TEM images of the corresponding nanofibers, which showed the thickness of the PDA sheath.

**Fiber Preparation.** Electrospinning on SSWs was similar to the previous study.<sup>26</sup> Electrospinning solution was prepared by dissolving 0.45 g of PS and 0.15 g of Pluronic F-127 in 6.0 mL of a mixed solvent of *N,N*-dimethylformamide and chloroform (1:1, v/v). The pumping speed for the electrospinning solution was 0.4 mL·h<sup>-1</sup>, and the distance and voltage between spinneret and SSW were 15.0 cm and 12 kV, respectively. The electrospinning duration was 2.5 min (Figure 1A). After electrospinning, dopamine hydrochloride was dissolved in the mixed solvent of Tri buffer (10 mM, pH = 8.5) and methanol (1:1, v/v); then, the SSWs coated with electrospun nanofibers were immersed in the dopamine solution (2.0 g·mL<sup>-1</sup>) for 12 h, twice (Figure 1B). Subsequently, the fibers were suspended in the vapor of 150 μL of aqueous GA solution (50%) at 50 °C for 12 h (Figure 1C). After that, the coating was extensively rinsed with deionized water and scratched with a knife to keep a 1.0 cm coating remaining at one end. The fiber was preconditioned by being soaked in static methanol under room temperature for 15 min prior to use.

**In Vivo SPME.** A fish was anaesthetized in dechlorinated municipal water containing 0.1% eugenol until loss of vertical equilibrium. Then, the steel needle (20 gauge) of a hypodermic syringe head was cut off and stabbed into the dorsal-epaxial muscle of the fish to a depth of about 1.5 cm. The custom-made fiber was inserted into the needle and reached to the end of the needle (Figure 2A). Subsequently, the needle was carefully withdrawn back to let the fiber be exposed in the muscle (Figure 2B). After a certain duration, the fish was reanaesthetized. The needle was put back to fish muscle under the guidance of the fiber to a depth of about 1.5 cm (Figure 2C). Then, the fiber was withdrawn from the needle, and the needle was removed (Figure 2D). The total sampling duration

was controlled to be 10 min. The fibers were then rinsed with deionized water and dried with a Kimwipe tissue. Subsequently, the fibers were desorbed in 80 μL of methanol for 30 min at a vortex rate of 400 rpm, and 20 μL of deuterated standards solution (50 ng·mL<sup>-1</sup>) was added as internal standard to calibrate the ionization efficiency for LC-MS/MS analysis. Two parallel samplings on both sides of the dorsal-epaxial muscle were carried out for mutual references.

**Liquid Extraction.** A fish was killed and approximately 100 mg of dorsal-epaxial muscle was collected in a centrifugation tube. Aliquots of 100 μL of ascorbic acid solution (0.1 M) and 400 μL of ice-cold methanol were added in the centrifugation tube; then, the tube was sonicated in an ice bath for 20 min and centrifuged at 3500 rpm for 30 min. The supernatant was transferred to an amber vial and dried under 60 °C in a nitrogen stream. The residue was dissolved in an aliquot of 200 μL of methanol, and 100 μL of the solution was transferred to the inset tube in an amber vial for LC-MS/MS analysis.

**Instrumental Analysis and Data Process.** The details for LC-MS/MS analysis are described in method S1 of the Supporting Information. All the data were processed with GraphPad Prism 5.

## RESULTS AND DISCUSSION

**Preparation and Characterization of the PDA Sheathed Nanofiber Coating.** PDA can be prepared by spontaneous polymerization of dopamine (DA) in Tri buffer, and it can form extremely thin layers on nearly all kinds of surfaces with thicknesses of up to dozens of nanometers.<sup>22</sup> However, compared with coating the outer surfaces, coating the stacked nanofibers is challenging since the inner pores could be blocked by the trapped air. In the previous studies, the inner



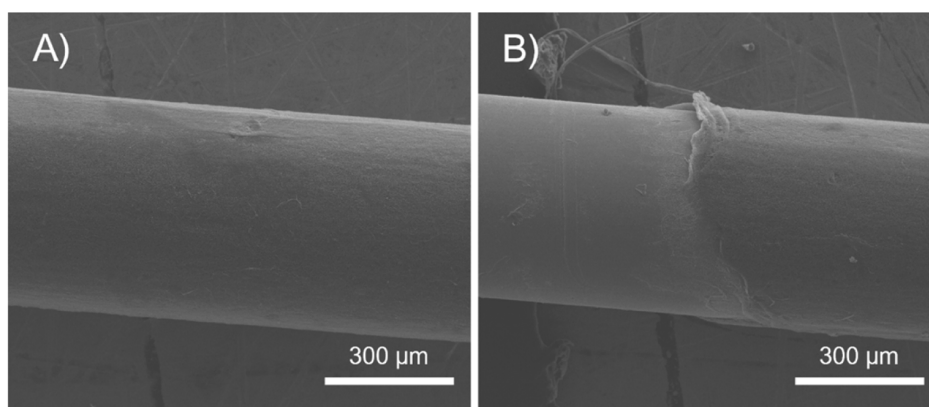


**Figure 4.** SEM images of PS@PDA-GA coating (A) and the interface of the coated and bare stainless steel wire (B).

surfaces were coated under the assistance of a vacuum pump,<sup>23</sup> or via pretreatment with plasma to improve surface hydrophilicity,<sup>25</sup> both of which permit DA aqueous solution to penetrate into the inner pores. However, these two methods were not convenient or straightforward enough as they required external equipment or an extra step to wash off plasma. In this study, Pluronic F-127, a water-soluble polymer, was applied in the electrospinning process by forming the hydrophilic sheath of the as-spun nanofibers to ensure the inner surfaces could be coated with PDA. The scanning electron microscopic (SEM) images of the as-spun nanofibers are shown in Figure 3A-1. By collecting the nanofibers on a plane collector, the contact angles were detected to be 0° (Figure 3B-1), which demonstrated the as-spun nanofibers were extremely hydrophilic. After 12 h of water washing, even though the dimensions of the nanofibers were not significantly changed (Figure 3A-2), the contact angles were dramatically increased to 104° (Figure 3B-2). Besides, C–O bonds could be detected via X-ray photoelectron spectroscopy (XPS) prior to water washing (Figure 3C-1), while only the signal of C–C bonds could be detected after 12 h of water washing (Figure 3C-2, Table S1, Supporting Information). All these phenomena confirmed emulsion electrospinning was occurring to form a core–sheath nanostructure, and the sheath was abundant with Pluronic F-127, while the core was abundant with PS.

In addition, methanol was mixed in Tri buffer to improve the permeability of DA solution, as methanol was capable of wetting the surface of PS even though the Pluronic F-127 sheath was dissolved during PDA sheathing (Figure 1B). The PDA sheath was successfully observed in the transmission electron microscopic (TEM) image after as-spun nanofibers were treated in DA solution, and byproduct PDA nanoparticles were observed (Figure 3A-3). Also, the contact angle was dramatically decreased to 78° after PDA sheathing (Figure 3B-3), and the signal of C–N bonds was detected as expected (Figure 3C-3). In the previous studies, hydrophilic sheaths originating from emulsion electrospinning or coaxial electrospinning were linear polymers;<sup>20,27</sup> thus, extra cross-linking procedures in the electrospun sheath are needed to enhance their durability to water and moisture.<sup>20,28</sup> However, cross-linking is cumbersome since the nanofibers would fuse during cross-linking.<sup>20,28</sup> Presently, only the in situ cross-linking protocol could effectively avoid the fusion of nanofibers.<sup>20</sup> On the contrary, sheathing with water-stable PDA after electrospinning is more convenient.

In order to enhance the strength of the electrospun architecture for facilitating direct sampling in semisolid tissue with the custom-made fibers, the nanofibers were cross-linked in GA vapor, as GA could react with PDA.<sup>29</sup> It was observed that the nanofibers were cross-linked at some sites (red circle in Figure 3A-4). Besides, the contact angle was nearly unchanged (80°) after GA cross-linking (Figure 3B-4). The percentage of C–O bonds increased after the nanofibers were suspended in GA vapor for 12 h (Table S1, Supporting Information), which also indicated that GA reacted with PDA. The nanofibers fusing significantly in the atmosphere with high moisture during GA cross-linking were not observed. Thus, the pore volumes in the coating would not be significantly decreased. The thickness of the coating was finally about 37 μm (Figure 4). It was notable that no surface defects were observed after being deployed in fish dorsal-epaxial muscle (Figure 4 and Figure S3, Supporting Information), which was due to GA cross-linking, as well as the protection of the syringe needle (Figure 2).

**In Vitro Evaluation of the PDA Sheathed Nanofiber Coating. Extraction Efficiency.** The extraction kinetics of the custom-made PS@PDA-GA fiber and another electrospun PS nanofibers coated SPME fiber were compared. The electrospun PS nanofibers coated SPME fibers were prepared by electrospinning PS solution (10% w/v, in *N,N*-dimethylformamide/chloroform 1:1 v/v; the electrospinning conditions were the same as the PS@PDA-GA fiber) without further sheathing and cross-linking steps. It was surprising that the extraction kinetics of PS fibers was faster than the PS@PDA-GA fibers for all analytes except for MEF (Figure 5), as PS coating could not be wetted in aqueous solutions (Figure S1, Supporting Information). On the other hand, it was found that the equilibrium extraction amounts in PS@PDA-GA fibers were more than ten times higher than those in PS fibers except for GEMF (4.4 times), even though the coating thicknesses were nearly the same for these two kinds of fibers. The possible reason for the fast extraction kinetics but low loading capacities of the PS fibers was that only a very thin layer of coating at the fiber surface was accessible to the analytes since the inner coating was blocked by the trapped air in the pores. On the contrary, since the PS@PDA-GA coating was wettable in aqueous solutions, the extraction kinetics of the PS@PDA-GA fibers was fast and their loading capacities were also high. It was highly remarkable that the positive charges on the surfaces of nanofibers were also suspected to affect the extraction of the ionizable pharmaceuticals. However, as the ratios of the equilibrium extraction amounts by using PS@PDA-GA nano-

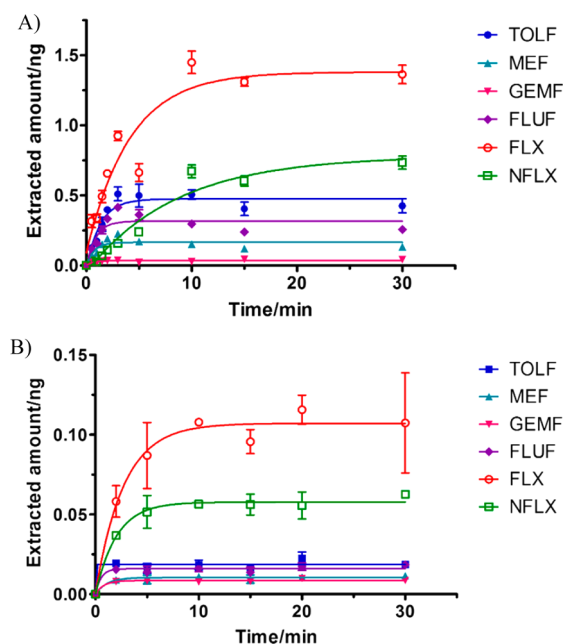


**Figure 5.** Extraction time profiles of pharmaceuticals with PS@PDA-GA fibers (A) and PS fibers (B). The concentration of each analyte in PBS buffer (pH = 7.4) was  $10 \text{ ng mL}^{-1}$ , and the agitation rate was 400 rpm. The extractions were conducted under room temperature. The error bars represented the standard deviations ( $n = 3$ ).

fibers to those by using nontreated PS nanofibers were not significantly different for acidic and basic pharmaceuticals (TOLF 23.7, MEF 14.7, GEMF 4.4, FLUF 18.4, FLX 11.3 and NFLX 12.5), we proposed that the positive charges on the nanofibers did not significantly affect the extraction capacities, and PS was the dominant extraction phase. The hydrophilic PDA sheath made the inner surfaces of the extraction phase accessible to the analytes, thus enhancing the extraction efficiencies.

Moreover, the extraction efficiency of the PS@PDA-GA coating was compared with polydimethylsiloxane (PDMS), previously used as the extraction phase for SPME of pharmaceuticals in fish dorsal-epaxial muscle,<sup>8</sup> fin,<sup>30</sup> and bile.<sup>31</sup> The preparation of the PDMS fibers was referred to in the previous studies, by mounting a piece of PDMS tubing (length 1.0 cm, O.D.  $640 \mu\text{m}$ , I.D.  $310 \mu\text{m}$ ) on a stainless steel wire (diameter  $480 \mu\text{m}$ ).<sup>8,30,31</sup> Figure 6 presented the extraction efficiencies of PS@PDA-GA fiber and PDMS fiber; the extraction efficiencies of the custom-made fiber were much higher than those of the PDMS fiber. Especially for TOLF, MEF, and FLUF, the normalized extracted amounts in the custom-made fibers were 26 to 42 times higher than those in PDMS fibers. Besides, the extraction kinetics of the PDMS fiber for FLX and NFLX in PBS buffer (pH = 7.4) recorded in the previous study<sup>31</sup> was also much slower than those of the PS@PDA-GA fiber.

**Biofouling Resistance.** The extraction phases used in biological matrices should be capable of resisting the adhesion of biological macromolecules on the surfaces. Otherwise, the adhered biological macromolecules would slow down the extraction kinetics by blocking the surfaces of the extraction phases and alter the ionization efficiencies when the macromolecules desorbed in the desorption solvents. It has been demonstrated that a hydrophilic surface could circumvent the adhesion of biological macromolecules by forming a thin water

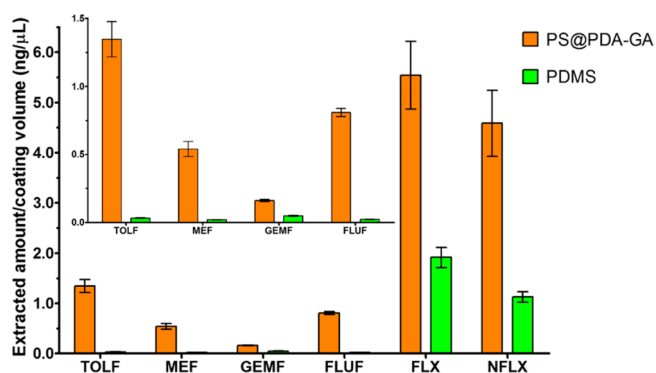


**Figure 6.** Comparison of the extraction efficiencies between PS@PDA-GA fibers and PDMS fibers. The inset provided an enlarged version of TOLF, MEF, GEMF, and FLUF. The concentration of each analyte in PBS buffer (pH = 7.4) was  $10 \text{ ng mL}^{-1}$ ; the agitation rate was 400 rpm, and the extraction time was 10 min. The error bars represented the standard deviations ( $n = 6$ ).

layer on it.<sup>20,27</sup> In this study, it was first observed through MALDI-TOF MS that there were no macromolecules in the desorption solvent of the PS@PDA-GA fiber exposed in blank fish muscle for 10 min (Figure S2, Supporting Information). Then, fibers exposed in blank fish muscle for 10 min and nonexposed fibers were desorbed in the desorption solvent; then, a series of standard solutions was added into the matrix-impacted and matrix-free solvents, and the ionization efficiencies of the matrix-free and matrix-impacted solution series were compared. As expected, there was no significant ionization bias observed in the matrix-impacted solutions compared with the matrix-free solutions (Table S2, Supporting Information).

**Intrafiber and Interfiber Reproducibility.** The intrafiber reproducibility and interfiber reproducibility were recorded in Table 1. It could be concluded from the intrafiber

**Table 1.** Intrafiber and Interfiber Reproducibility of PS@PDA-GA Fiber ( $n = 6$ ) and Limits of Detection (LOD, S/N = 3,  $\text{ng g}^{-1}$ ) of in Vivo SPME in Fish Dorsal-Epaxial Muscle

	TOLF	MEF	GEMF	FLUF	FLX	NFLX
intrafiber	6.4%	4.8%	4.6%	3.8%	4.1%	7.3%
interfiber	9.7%	10.2%	5.8%	5.9%	12.2%	14.3%
LOD	2.3	1.1	6.3	6.7	8.9	6.6

reproducibility that the PS@PDA-GA fiber was stable for six sampling-desorption cycles, which was superior to the nanofibrous sorbent whose hydrophilic sheath was not stable in aqueous phases.<sup>25</sup> The interfiber reproducibility was also satisfactory.

**In Vivo Sampling Pharmaceuticals in Fish Muscle.** The deployment of PS@PDA-GA fibers in fish dorsal-epaxial muscle has been described above and shown in Figure 2. The in vivo sampling duration was as short as 10 min, while the sensitivities were quite satisfactory (Table 1). Bioconcentration of GEMF was previously observed to be very low in fish muscle (bioconcentration factors in the range of 0.2–0.6).<sup>30</sup> In this study, the four acidic pharmaceuticals in fish muscle were also detected to be low and even could not be detected with the liquid extraction (LE) method (Table S3, Supporting Information). Therefore, only FLX and its metabolite NFLX were quantified in fish muscle with in vivo SPME. The

sampling-rate calibration method<sup>8</sup> was adopted to quantify the concentrations of FLX and NFLX in fish exposed to FLX at the nominal concentration of  $2.0 \mu\text{g}\cdot\text{L}^{-1}$ . The sampling rates were recorded in another group of fish exposed to FLX at the nominal concentration of  $10.0 \mu\text{g}\cdot\text{L}^{-1}$  (Table S4, Supporting Information). It was observed in Figure 7 that the mean concentrations in six fish determined with in vivo SPME and LE were very close to each other, which demonstrated the excellent accuracy of in vivo SPME.

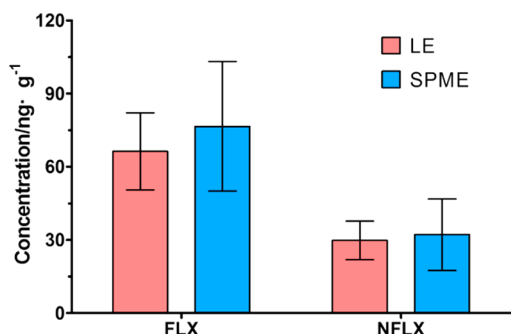


**Figure 7.** Mean concentrations of FLX and NFLX in dorsal-epaxial muscle of the six fish determined with LE and in vivo SPME; the error bars represented the standard deviations ( $n = 6$ ).

## CONCLUSIONS

In this study, a facile substitution methodology was proposed to sheath electrospun nanofibers for in vivo SPME of pharmaceuticals in fish muscle. In this methodology, the water-soluble sheath of emulsion electrospun PS@Pluronic F-127 core–sheath nanofibers was substituted with self-polymerized PDA. Pluronic F-127 sheath was originally introduced to enhance the wettability of the as-spun networks to promote PDA sheathing efficiency. Compared with the previous protocols of coating microfibers and nanofibers under the assistance of vacuum pump or via pretreatment with plasma, the one-step substitution process was more convenient and straightforward. Besides, different from cross-linking in water-soluble sheath to enhance water stability,<sup>20</sup> the substitution of water-soluble sheath with water-stable sheath provided a new way of preparing water-stable hydrophilic sheath. In addition, the self-polymerized PDA sheath in this study was much less expensive than the cross-linked collagen sheath.<sup>20</sup>

The extraction efficiency of the novel coating was much higher than the previously used thicker PDMS coating and the nonsheathed electrospun PS nanofiber coating. The coating was stable for several repeat sampling-desorption cycles and exhibited excellent interfiber reproducibility and antibiofouling ability. Due to the direct sampling of pharmaceuticals in fish dorsal-epaxial muscle, satisfactory sensitivity and accuracy were achieved. Overall, this novel PS@PDA-GA fiber is promising to be used for in vivo sampling, due to its rapid sampling kinetics, low cost, and easy preparation procedure.

## ASSOCIATED CONTENT

### Supporting Information

LC-MS/MS analytical parameters, water contact angle of PS nanofibers, MOLDI-TOF MS analysis results, SEM images of the used PS@PDA-GA fiber, percentages of covalent bonds in the nanofiber surfaces, regression slopes of curves derived from

the matrix-free and matrix-impacted solutions, concentrations determined with liquid extraction, limits of detection of liquid extraction, and sampling rates of FLX and NFLX. This material is available free of charge via the Internet at <http://pubs.acs.org>.

## AUTHOR INFORMATION

### Corresponding Authors

\*Tel./Fax: +86-20-84110845. E-mail: cesoygf@mail.sysu.edu.cn.

\*Tel./Fax: +86-20-84110845. E-mail: jiangrfs@mail.sysu.edu.cn.

### Notes

The authors declare no competing financial interest.

## ACKNOWLEDGMENTS

We acknowledge financial support from the projects of NNSFC (21225731, 21477166, 21407184) and the NSF of Guangdong Province (S2013030013474).

## REFERENCES

- (1) Ouyang, G.; Vuckovic, D.; Pawliszyn, J. *Chem. Rev.* **2011**, *111*, 2784–2814.
- (2) Musteata, M. F.; Musteata, M. L.; Pawliszyn, J. *Clin. Chem.* **2008**, *52*, 708–715.
- (3) Xu, J.; Luo, J.; Ruan, J.; Zhu, F.; Luan, T.; Liu, H.; Jiang, R.; Ouyang, G. *Environ. Sci. Technol.* **2014**, *48*, 8012–8020.
- (4) Vuckovic, D.; de Lannoy, I.; Gien, B.; Shirey, R. E.; Sidisky, L. M.; Dutta, S.; Pawliszyn, J. *Angew. Chem., Int. Ed.* **2011**, *50*, 5344–5348.
- (5) Cudjoe, E.; Bojko, B.; de Lannoy, I.; Saldivia, V.; Pawliszyn, J. *Angew. Chem., Int. Ed.* **2013**, *52*, 12124–12126.
- (6) Zhang, X.; Es-haghi, A.; Musreata, F. M.; Ouyang, G.; Pawliszyn, G. *Anal. Chem.* **2007**, *79*, 4507–4513.
- (7) Zhang, X.; Oakes, K. D.; Luong, D.; Metcalfe, C. D.; Pawliszyn, J.; Servos, M. R. *Anal. Chem.* **2011**, *83*, 2371–2377.
- (8) Ouyang, G.; Oakes, K. D.; Bragg, L.; Wang, S.; Liu, H.; Cui, S.; Servos, M. R.; Dixon, D. G.; Pawliszyn, J. *Environ. Sci. Technol.* **2011**, *45*, 7792–7798.
- (9) Zhang, X.; Oakes, K. D.; Luong, D.; Wen, J. Z.; Metcalfe, C. D.; Pawliszyn, J.; Servos, M. R. *Anal. Chem.* **2010**, *82*, 9492–9499.
- (10) Zhang, X.; Oakes, K. D.; Luong, D.; Metcalfe, C. D.; Servos, M. R. *Anal. Chem.* **2011**, *83*, 6532–6538.
- (11) Ai, J. *Anal. Chem.* **1997**, *69*, 1230–1236.
- (12) Jiang, R.; Pawliszyn, J. *Trends Anal. Chem.* **2012**, *39*, 245–253.
- (13) Tian, J.; Xu, J.; Zhu, F.; Lu, T.; Su, C.; Ouyang, G. *J. Chromatogr. A* **2013**, *1300*, 2–16.
- (14) Xu, J.; Zheng, J.; Tian, J.; Zhu, F.; Zeng, F.; Su, C.; Ouyang, G. *Trends Anal. Chem.* **2013**, *47*, 68–83.
- (15) Zhang, W.; Sun, Y.; Wu, C.; Xing, J.; Li, J. *Anal. Chem.* **2009**, *81*, 2912–2920.
- (16) Chambers, S. D.; Holcombe, T. W.; Svec, F.; Fréchet, J. M. J. *Anal. Chem.* **2011**, *83*, 9478–9484.
- (17) Sharifi, S.; Behzadi, S.; Laurent, S.; Forrest, M. L.; Stroeve, P.; Mahmoudi, M. *Chem. Soc. Rev.* **2012**, *41*, 2323–2343.
- (18) Xia, T.; Hamilton, R. F., Jr.; Bonner, J. C.; Crandall, E. D.; Elder, A.; Fazlollahi, F.; Girtsman, T. A.; Kim, K.; Mitra, S.; Ntim, S. A.; Orr, G.; Tagmount, M.; Taylor, A. J.; Telesca, D.; Tolic, A.; Vulpe, C. D.; Walker, A. J.; Wang, X.; Witzmann, F. A.; Wu, N.; Xie, Y.; Zink, J. I.; Nel, A.; Holian, A. *Environ. Health Perspect.* **2013**, *121*, 683–690.
- (19) Bonner, J. C.; Silva, R. M.; Taylor, A. J.; Brown, J. M.; Hilderbrand, S. C.; Castranova, V.; Porter, D.; Elder, A.; Oberdörster, G.; Harkema, J. R.; Bramble, L. A.; Kavanagh, T. J.; Botta, D.; Nel, A.; Pinkerton, K. E. *Environ. Health Perspect.* **2013**, *121*, 676–682.
- (20) Wu, Q.; Wu, D.; Guan, Y. *Anal. Chem.* **2013**, *85*, 11524–11531.
- (21) Yarin, A. L. *Polym. Adv. Technol.* **2011**, *22*, 310–317.
- (22) Lee, H.; Dellatore, S. M.; Miller, W. M.; Messersmith, P. B. *Science* **2007**, *318*, 426–430.

- (23) Ryu, J.; Ku, S. K.; Lee, H.; Park, C. B. *Adv. Funct. Mater.* **2010**, *20*, 2132–2139.
- (24) Hu, H.; Yu, B.; Ye, Q.; Gu, Y.; Zhou, F. *Carbon* **2010**, *48*, 2347–2353.
- (25) Xie, J.; Zhong, S.; Ma, B.; Shuler, F. D.; Lim, C. T. *Acta Biomater.* **2013**, *9*, 5698–5707.
- (26) Zewe, J. W.; Steach, J. K.; Olesik, S. V. *Anal. Chem.* **2010**, *82*, 5341–5348.
- (27) Wu, Q.; Wu, D.; Guan, Y. *Anal. Chem.* **2013**, *85*, 5924–5932.
- (28) Destaye, A. G.; Lin, C.-K.; Lee, C.-K. *ACS Appl. Mater. Interfaces* **2013**, *5*, 4745–4752.
- (29) Sureshkumar, M.; Lee, C.-K. *Carbohydr. Polym.* **2011**, *84*, 775–780.
- (30) Zhang, X.; Oakes, K. D.; Cui, S.; Bragg, L.; Servos, M. R.; Pawliszyn, J. *Environ. Sci. Technol.* **2010**, *44*, 3417–3422.
- (31) Togunde, O. P.; Oakes, K. D.; Servos, M. R.; Pawliszyn, J. *Environ. Sci. Technol.* **2012**, *46*, 5302–5309.